

Design and Development of a Novel Vapor Recompression Distillation Unit for Bio Ethanol Manufacturing Process

R.H. Rathnayake, I.B. Wijethunga and E.P.R.H.H.W. Nilmalgoda*

Department of Biosystems Technology, Faculty of Technology, Sabaragamuwa University of Sri Lanka, Belihuloya, 70140

*Corresponding Author

DOI: <https://doi.org/10.51584/IJRIAS.2024.911033>

Received: 01 November 2024; Accepted: 09 November 2024; Published: 12 December 2024

ABSTRACT

Bioethanol is an environmentally friendly fuel source that offers significant advantages over fossil fuels, including lower emissions and sustainability. However, conventional distillation methods in bioethanol production are often associated with high energy consumption and inefficiencies. This research introduces a novel vapor recompression distillation unit, designed and fabricated to optimize the bioethanol manufacturing process. Addressing the high energy demands of traditional methods, this study proposes vapor recompression batch distillation as a more energy-efficient and effective solution, enhancing both the sustainability and productivity of bioethanol production. The system consists of two main units: a primary reactor and a calandria reactor, equipped with two programmable control mechanisms. To assess the performance and efficiency of the vapor recompression distillation unit, batch distillation experiments were conducted, measuring variables such as reactor vapor pressure, temperature, vapor flow rate, calandria reactor temperature, and the coefficient of performance (COP). Three distinct ethanol mixtures, derived from Sugar, Jackfruit, and Ice Cream Beans, were prepared as feedstock for the distillation process. Consistent water and yeast amounts were maintained across all mixtures, which were distilled over a period of approximately three hours. Key parameters including pH, electrical conductivity, density, and both kinetic and dynamic viscosity were analyzed for the first effect distillation samples. The study revealed a COP of 1.9851, indicating satisfactory distillation capability. The average conversion efficiency of the system was 25.89% in the first effect, with the Sugar solution achieving the highest ethanol concentration at 22.0%, and the Jackfruit sample the lowest at 18.1%. These results demonstrate the feasibility of using this system for ethanol distillation, significantly reducing both processing time and energy consumption.

Keywords: Ethanol, Vapor recompression distillation, Sustainability, Innovation, coefficient of performance

INTRODUCTION

Ethanol is a versatile and widely used compound with applications ranging from biofuel production to the pharmaceutical and beverage industries (Bušić et al., 2018) (Canales & Marquez, 1992). Derived from the fermentation of sugars or renewable resources like corn and sugarcane, ethanol plays a crucial role in sectors such as fuel, industrial processes, and medicine. As a renewable energy source, it contributes to efforts aimed at reducing reliance on fossil fuels (Uday Bhaskar Babu & Jana, 2014) (Tgarguifa et al., 2017). With ethanol derived from renewable sources, it reduces greenhouse gas emissions, lessens dependence on finite fossil fuels, and stimulates domestic economies (Vohra et al., 2014). Ethanol E-fuel signifies a significant step toward cleaner, more sustainable transportation solutions (Hargono et al., 2021) (Dias & Modesto, 2011).

Conventional ethanol distillation is a process used to separate ethanol from water and other components in a fermented solution. This method is commonly employed in the production of ethanol for various purposes, including the beverage industry, industrial applications, and biofuel production (Ansari et al., 2016) (Gavahian et al., 2019). The major components include the distillation column, boiler, condenser, trays or packing materials, reflux system, collection vessels, and refinement equipment. Conventional ethanol distillation involves several key processes (Uday Bhaskar Babu & Jana, 2014). The process begins with a fermented solution containing ethanol, water, and by-products from microbial fermentation. This mixture is heated in a boiler, and the resulting vapors ascend through a distillation column equipped with trays or packing materials. These components

facilitate the separation of ethanol from water and impurities based on differences in boiling points (Singh & Rangaiah, 2017) (Errico & Rong, 2012). The condensed ethanol vapors, known as distillate, are collected at various levels in the column. Some setups may incorporate a reflux system to enhance separation. The final product is collected in vessels and may undergo further refinement for desired purity (Arshad et al., 2017). Conventional ethanol distillation, despite its widespread use, presents several drawbacks. The process is notably energy-intensive, requiring substantial input for heating and vaporization (Duque et al., 2021). This not only contributes to higher production costs but also raises environmental concerns due to increased energy consumption (Duque et al., 2021) (Rosales-Calderon & Arantes, 2019). Additionally, the lower boiling point of ethanol compared to water poses a challenge in achieving high ethanol concentrations efficiently, necessitating additional energy. Water usage is another consideration, as the distillation process involves significant water usage for cooling and condensation (Das et al., 2013) (Christian Oseto, 2020). Disposal and handling of by-products, such as yeast and solids generated during fermentation, add complexity to the overall process. The limited purity achieved through conventional distillation may require supplementary purification steps for certain industrial or fuel applications (Aditya et al., 2016). Moreover, the potential emission of Volatile Organic Compounds (VOCs) during distillation raises both environmental and safety concerns (Duque et al., 2021) (El-Sheekh et al., 2022).

Vapor recompression distillation column (VRC) stands out as a superior alternative to conventional ethanol distillation, particularly in terms of energy efficiency, sustainability, reducing carbon footprint and process optimization (Arifeen et al., 2007) (Gavahian et al., 2019). This method addresses the substantial energy demands associated with distillation by recycling vapor within the system (Ishola et al., 2013) (Kazemi et al., 2016). The process involves heating a fermented solution to generate vapor containing ethanol. Instead of condensing this vapor into liquid form and discarding it, the VRC system utilize compressors to increase its pressure (Hargono et al., 2021) (Gavahian et al., 2016). The compressed vapor is then reintroduced into the secondary reactor, elevating the internal temperature. This augmented temperature enhances the separation of ethanol from water and impurities within the secondary reactor, reducing the need for additional external heat (Singh & Rangaiah, 2017) (Sarkar et al., 2012). By reusing vapor and avoiding its condensation, the VRC system significantly minimizes energy consumption, making the ethanol production process more sustainable and economically viable. Moreover, it enables a more continuous and efficient distillation process compared to traditional methods (Galbe et al., 2007) (Santos et al., 2018).

Automation in the ethanol distillation maximizes the product recovery compared with conventional distillation method (Li et al., 2021) (Palacios-Bereche et al., 2014) (Dias & Ensinas, 2009) . The main objective of the present study was to design a novel high efficiency automated VRC unit for fuel grade bio ethanol manufacturing process. The automated Programmable Logic Controller (PLC) setup continuously monitors and adjusts parameters such as temperature, pressure, and flow rates for high precision and reliability of the process (Enweremadu & Rutto, 2010) (Chen et al., 2021). This ensures an efficient vapor recompression process, where compressors, valves, blowers and other components are automatically operated using pre-programmed instructions to recycle vapor within the system optimally. Moreover, this system also allows for remote monitoring and control, enabling operators to manage the distillation process from a centralized location. Fault detection, diagnostics, and data logging features results high system performance and provide valuable insights for process optimization. At the later part of the study, the efficiency of the vapor recompression distillation unit was determined by a pilot study using three types of feedstock solutions. This approach aims to determine the economic and technical feasibility of VRC system in bio ethanol production.

MATERIAL AND METHODS

Figure 1 summarizes the overall methodology of the study.

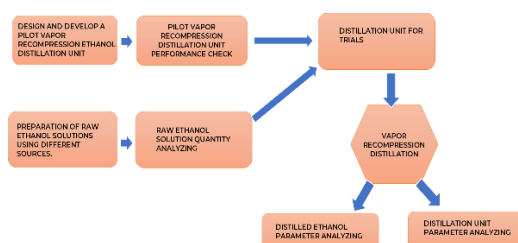


Figure 1: Summary of the study methodology

Basic design components and their functions

The vapor recompression ethanol distillation unit utilized in this research is comprised of several critical components designed for efficient separation and purification. The main reactor and calandria reactor form the core distillation apparatus, complemented by the CR isolation valve and vapor-liquid separator to facilitate precise control over the distillation process. Each component is constructed using materials selected for their corrosion resistance and thermal stability, ensuring durability under the demanding conditions of ethanol distillation. The air emitter and high-pressure blower are instrumental in maintaining optimal pressure conditions, while the feed pump and circulate compressor contribute to the controlled circulation and introduction of ethanol. The ethanol feed intake and outlet components play a pivotal role in managing the entry and exit of ethanol throughout the distillation stages, emphasizing the importance of materials compatible with ethanol to uphold the unit's operational integrity.

The main reactor

The main reactor employed in this vapor recompression ethanol distillation unit features a capacity of 25 liters and is constructed using 2mm mild steel sheet. This reactor is equipped with multiple outlet ports, facilitating various functions crucial to the distillation process. Six outlet ports are incorporated into the reactor design to enable multipurpose functionality. One port serves as the inlet for introducing the raw ethanol feed solution. Two additional outlet ports are dedicated to supplying agitation airflow, which is connected to a circulating compressor. This compressor generates fully dried airflow to agitate the raw solution effectively. Another outlet port is utilized to maintain air pressure equilibrium between the main reactor and the circulating compressor. The primary outlet of the reactor is directly linked to the CR isolation valve, while a bottom outlet port connects to the calandria reactor for recirculating the ethanol solution. Internally, the main reactor is equipped with an induction-type heater. Operating at a voltage of 56V, this heater is capable of reaching its maximum set point within a stable amp range. Consisting of a 250g stainless steel block, the induction heater generates heat through inductive power, which is then transferred to the raw solution via the stainless-steel block. Control of the induction heater is achieved through a 4mA to 20mA analog signal using a Siemens LOGO 24CE PLC unit. This signal regulates the PWM cycle of the IGBT switches within the induction heater. A 25% duty cycle is generated when the control signal reaches 4mA, increasing to 50% between 5mA to 11mA, 75% between 12mA to 16mA, and reaching 100% duty cycle when the control signal ranges from 17mA to 20mA. Temperature monitoring within the reactor is facilitated by one PT100 TRD type sensor and two Class E type thermocouples. These thermocouples are calibrated using a Fluke 550E thermocouple calibrator at room temperature and 100 degrees Celsius. With a sheath diameter of approximately 5mm, both thermocouples are mounted using brass nuts and insulated using heat compound to increase the thermal conductivity between the thermocouple and the solution. These sensors relay temperature data to an amplifier before being archived in the PLC unit for analysis. To minimize heat losses during operation, the exterior surface of the reactor is covered with 8mm thick glass wool insulation.

The calandria reactor

The calandria reactor, serving as the secondary reactor in this distillation unit, is crafted from 2mm mild steel, ensuring robustness and compatibility with ethanol processing. It is assembled using forty bolts (10mm) for the top joint and MIG welding for the bottom part joints. Structurally, the reactor is divided into three sections: the low-pressure section, the rectification section, and the cooling section. The main inlet of the reactor is linked to the CR isolation valve, while two additional inlets are connected to a high-pressure blower. Low pressure section of the reactor maintains a minimized pressure condition, facilitating the easy flow of vapor streams. This low-pressure condition is sustained with the aid of the high-pressure blower, and this section is separated from other sections by a copper plate that consists of three-hundred holes ($d=5\text{mm}$). The rectification section is equipped with a secondary heater element made out of nichrome wires to elevate the temperature of the vapor stream. Output from this section is directly channeled to the vapor-liquid separator via two outlet ports. The final section of the calandria reactor functions as a cold reservoir, with one end connected to the vapor-ethanol separator and the other to the main reactor. Temperature monitoring within the reactor is facilitated by six Class E type thermocouples, all strategically placed and connected to the MURRELEKTRONIK 440R2 D/A converter which efficiently converts analog signals to digital signals with a stable 0.01 resolution. All thermocouples are calibrated using a Fluke 550E thermocouple calibrator for accuracy. The temperature signals are then

transmitted to indicators for monitoring purposes. Additionally, a SENSHI 8R7 differential pressure transmitter is employed to sense the pressure levels in both the lower and rectification sections of the Calandria reactor. These pressure signals are received by the LOGO 24CE PLC unit for further processing.

CR isolation valves

The CR isolation valve serves as the pivotal link between the main reactor and the calandria reactor in the system. The valve which is a four-inch section with a diameter of 100mm, is equipped with an internal electromagnetic actuator responsible for controlling the valve position, with its operation dependent on the pressure within the Calandria reactor and the temperature of the main reactor. A differential pressure flow transmitter installed on one side of the valve facilitates the calculation of vapor flow rates between the two reactors. Constructed entirely of stainless steel, the valve body ensures durability and resistance to corrosion. Each outlet of the valve is connected using two flanges for secure sealing. Internal valve actuation is governed by digital commands supplied by the LOGO 24CE PLC unit, ensuring accurate and responsive control. Two limit switches are incorporated into the valve mechanism to detect its position, enhancing operational safety and control. The normally open (N/O) pin of the first limit switch is connected to the normally closed (N/C) pin of the second limit switch, and vice versa, to form a loop. The detector rods of all limit switches are connected to the cam shaft of the CR isolation valve. The magnetic converter offers three-wire control modes for advanced control: the combination of positive (+) and ground (G) wires opens the valve, while negative (-) and ground (G) wires close it. Positive (+) and negative (-) wires can pause the position of the CR isolation valve. Each control requires 5V command signals from the LOGO 24CE PLC. To minimize heat loss, the valve body is insulated with an 8mm layer of glass wool. This comprehensive design ensures efficient and reliable operation of the CR isolation valve within the reactor system.

The water-ethanol separator

The water ethanol separator plays a critical role in separating ethanol from the vapor stream. Constructed from 2mm mild steel, this cylindrical apparatus houses eight Peltier mounted to a 4mm copper block plate. All plates are powered by a 12V 5A constant amperage SMPS power supply which operates at 12V with a capacity of 50A and features active rectification. Following the rectification section of the calandria reactor, high-temperature ethanol vapor is directed into the separator unit. Utilizing a high-pressure blower, the vapor stream impacts the copper block within the separator. The mounted Peltier plates can cool the plate surroundings to approximately -4 degrees Celsius. The hot side of the Peltier plates is cooled down using fin-type aluminum heat sinks. After the separation process, the cooled ethanol is directed to the third section of the calandria reactor via gravitational force. Within the separator, a PT100 RTD is employed to measure temperature, and it transmits temperature data to the programmable MCU and indicators for monitoring purposes and the pressure transmitter monitors the high- pressure blower pressure. Inlet and outlet ports of the separator are 50mm in diameter, connected to the calandria reactor using two hex nipple joints. Similar to other units, the separator is insulated with an 8mm layer of glass wool to minimize heat loss during operation.

The high-pressure blower

The high-pressure blower serves as a crucial component of the Calandria reactor, providing a constant supply of high-pressure air to the rectification section. Equipped with a high-pressure impeller containing 30 blades, this blower is driven by a 48V BLDC motor control system capable of exceeding a maximum RPM of 13,000. RPM control is managed by a BLDC motor control unit, which receives a 0 to 5V analog signal command from the LOGO 24CE PLC unit. This signal dynamically adjusts the blower rotation speed in response to fluctuations in vapor stream flow rate. The input and output pipes of the impeller are constructed from PVC and connected using plastic flanges. An encoder pointer inside the impeller facilitates the measurement of RPM. To measure blower pressure, a differential pressure transducer is installed at the end of the blower output pipe and at the Calandria inlet port. Additionally, the blower is mounted to the vapor-liquid separator to mitigate vibration.

The recirculate compressor

The recirculate compressor plays a crucial role in balancing the air pressure between two reactors and atmospheric pressure within the system. Its function is particularly vital during the operation of the Calandria

reactor, where pressure levels can fluctuate, potentially affecting the boiling point of ethanol. By utilizing this compressor, such fluctuations can be mitigated, ensuring stable operating conditions. Powered by a 230V main supply, the rotary compressor is controlled via a magnetic contactor, with supply governed by a pre-programmed MCU. This compressor is a modified rotary type obtained from an old air conditioner, is capable of rotating in both directions determined by the data of the MCU. Following modification, the inlet ports were enlarged to accommodate increased inlet pipe diameters. The outlet pipe is directly connected to the air emitter. To enhance insulation, the inlet pipes are insulated using an 8mm glass wool layer, and all pipes are connected using 25mm hex nipples. This comprehensive setup ensures efficient and reliable operation of the recirculate compressor within the reactor system.

The feed pump

The feed pump, which is a one horsepower centrifugal pump, is essential for supplying the raw ethanol solution to the main reactor. Its suction side is connected to a non-return PVC valve, ensuring a constant liquid quantity within the pump. The outlet of the feed pump is directly connected to the main reactor. Control of the feed pump is managed by an ANLY 60 level controller and a magnetic contactor. Typically, it is programmed to cut off when the liquid level reaches 13 liters of raw ethanol solution. This setup ensures precise and reliable feeding of the ethanol solution into the main reactor, maintaining optimal operating conditions.

The air emitter

The air emitter serves the crucial function of controlling the bad odor mixed with the compressed air resulting from the reactor operation. Following the completion of the reactor process, residual water solutions often emit unpleasant odors. To address this, the air emitter utilizes sponge filtering media and granular activated carbon as absorbents. Housed within a cylindrical apparatus, the air emitter contains these filtering agents to effectively absorb odorous compounds. With a bore diameter of 120mm and a length of 400mm, the air emitter features a single inlet port connected to the recirculate compressor via a 50mm PVC pipe. This comprehensive design ensures efficient odor control by effectively filtering the compressed air before emission.

System configuration

The vapor recompression ethanol distillation unit is entirely reliant on Programmable Logic Controller unit (PLC) and Microcontroller unit (MCU). Each component is capable of functioning with the control signals from the MCU and PLC. Certain components of the system have separate power supplies to minimize electrical noise during initial startup after prolonged shutdown periods. Figure 2 illustrates the reception and transmission of data, as well as the generation of sensor data within the system.

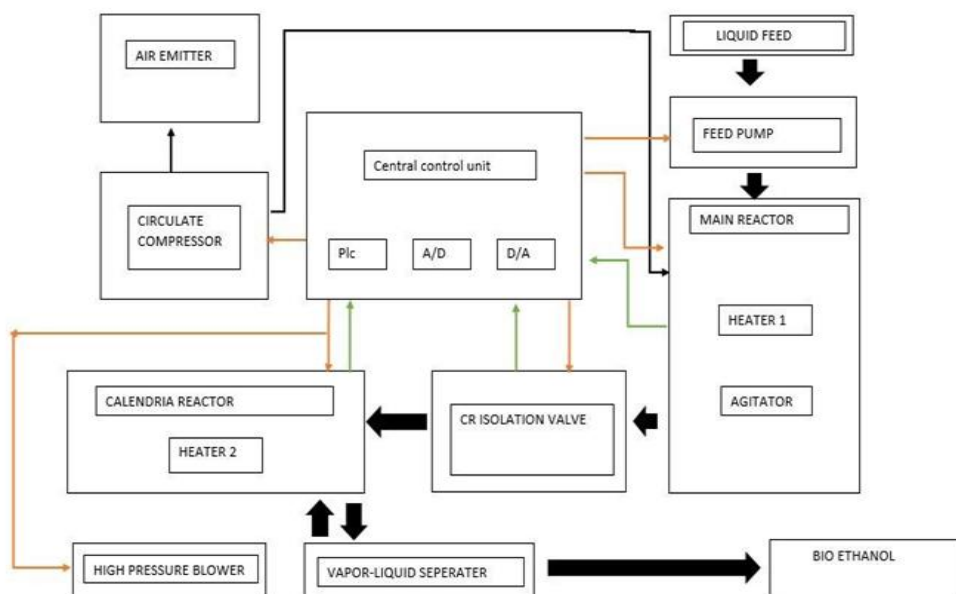


Figure 2. Transmission and reception of data

Programmable logic controller (PLC)

A Programmable Logic Controller (PLC) serves as a robust computing system which assimilates incoming data, subsequently initiating outputs based on predefined parameters. The PLC operates at a working voltage of 24V DC, necessitating a 24V 5A SMPS power supply and is capable of handling both digital and analog inputs and outputs. The LOGO Soft Comfort software is utilized for programming the PLC where it offers three programming methods namely ladder programming (LAD), functional block programming (FBD), and UDF diagram. Ladder programming is used in this experiment because of its simplicity. With the capacity to control 400 specific functions, it boasts 8 inputs and 4 digital transistor outputs, along with special short-circuit protection function. It features a display unit for basic programming and is mounted on the 39mm DIN rail of the metal enclosure panel of the unit. The input and output modules that establish connectivity with the machinery, facilitates the data transmission to the CPU which facilitates tailored outcomes.

Micro controller unit (MCU)

Preprogrammed MCU is required to control continuous mode equipment. SS MB 1.1 version microcontroller board is utilized in this setup for high-precision analytical and arithmetic operations. The core controller is the 32MX320 chip, offering several advantages compared to other PIC series controllers. This MCU boasts a clock speed of 80MHz and features a 32-bit MIPS M4K Core with a 5-stage pipeline. Methods include a shift register array, with a hardware array system capable of overwriting multiple program codes within a single array. The MIPS16e mode is utilized to reduce program code size, resulting in a 40% savings in local memory. Additionally, it is equipped with 32 x 32-bit Core Registers and 32 x 32-bit Shadow Registers to retain previously used data. With 256K Flash (plus 12K boot Flash) and 32K RAM (capable of executing from RAM), it can handle very large codes. Internally, it features a 4-channel Hardware DMA Controller and a Flash module with a capacity of 256 bytes, allowing instructions or data to be locked in cache for fast access. Furthermore, it includes 2 internal oscillators (8 MHz & 31 kHz) for serial arithmetic operations. A Watchdog Timer with a separate RC oscillator is employed to monitor high-precision time delays during the distillation process. Additionally, it offers a 2-wire programming and debugging interface for easy programming of the microcontroller unit.

Preparation of raw solutions

To analyze the performance and efficiency of the vapor recompression ethanol distillation unit, a batch distillation process was conducted. Three different raw ethanol solutions were prepared for this study. Across all three solutions, the water and the yeast amounts were identical. Sugar, Jackfruit, and Ice cream beans were used as feedstock to prepare the raw ethanol mixture. The container was initially washed using hot water before mixing the feedstock in measured amount of water and finally yeast was added. The container was then air locked using a water bath and a saline tube was fixed to the container to remove the carbon dioxide from the setup. The setup was then transferred to a dark place to facilitate fermentation process. All three samples were prepared in the same day and were kept for 5 days for the fermentation to be completed. The composition of the three solutions is presented in Table 2. Subsequently the three solutions were fed into the distillation unit and kept around 3 hours for the distillation process to be complete.

Table 1. Composition of raw solutions

	Solution 01	Solution 02	Solution 03
Filtered water	15 liters	15 liters	15 liters
Feedstock	White sugar (5 kg)	Jackfruit (5 kg)	Cream beans (5 kg)
Yeast	125 g	125 g	125 g

Data collection

Using the pilot-scale vapor recompression ethanol distillation unit (Figure 3), temperature, pressure and flow rate data were obtained using sensors and indicators. Temperature data included the main reactor and calandria reactor temperature whereas pressure data included main reactor vapor pressure. Additionally, main reactor

output flow rate was measured. Moreover, the produced ethanol was measured using a measuring flask within a specific time.



Figure 3. Fabricated Vapor recompression system

Parameter Estimation

Main reactor vapor pressure analyzing

The Antoine equation emerges as a crucial component in establishing the relationship for ethanol vapor in the vapor recompression distillation unit (Vacuubrand, 2018). This empirical equation, derived from thermodynamic principles, provides a mathematical framework for predicting the vapor pressure of ethanol as a function of temperature. By incorporating the Antoine equation (Equation 1) into the experimental framework, researchers can accurately model and analyze vapor phase behavior, thereby enhancing process control and optimization efforts.

$$\log_{10}(P) = A - \left[\frac{B}{T+C} \right] \quad \text{Equation 1}$$

P = Vapor pressure (mmHg)

T = Temperature (K)

A, B and C = Coefficient values for ethanol 18.99, 3846.25 and -40.191 respectively for temperature range 273 to 351 K.

Coefficient of Performance analyzing

The Coefficient of Performance (COP) is a key metric for assessing the energy efficiency of the vapor recompression distillation unit. It represents the ratio of useful heating or cooling output to the energy input required to drive the system. For distillation processes, a higher COP indicates greater efficiency in utilizing energy for ethanol recovery.

The COP of the distillation unit was evaluated by measuring the energy input versus the energy effectively utilized in the vapor recompression process. Data on primary variables—vapor pressure, temperature, vapor flow rate, and calandria reactor temperature—were collected throughout the batch distillation process. The COP was calculated using the following equation 2.

$$COP = \frac{\text{Useful energy output } (Q)}{\text{Energy input } (W)} \quad \text{Equation 2}$$

where:

- **Q** is the heat energy absorbed in the calandria reactor, which contributes directly to the ethanol distillation process.

- **W** is the electrical energy consumed by the compressor and control systems.

RESULTS AND DISCUSSION

Temperature sequence in the main reactor

Temperature monitoring within the main reactor is facilitated by one RTD sensor and two thermocouples. Temperature monitoring and control are essential for ensuring optimal reaction kinetics and product quality. According to the temperature data, there is a gradual increment of temperature data in all three types of sensors where thermocouple 02 indicates a higher value compared to other sensors. According to the data, the temperature of 353 K (80°C) could be obtained in around 3 hours of distillation time. Temperature sequence values are illustrated in Figure 4.

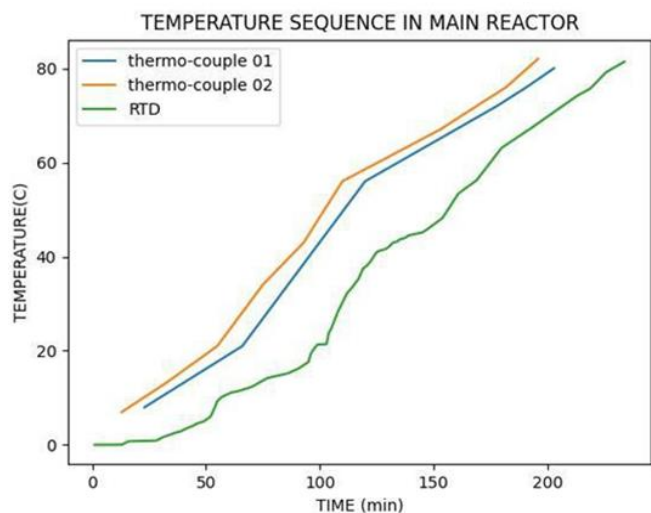


Figure 4. Temperature sequence of the main reactor

Changes in vapor pressure with the changing temperature in the main reactor

As described by many researchers, the Antoine equation is adopted to calculate the ethanol vapor pressure within the main reactor (Janousek, 2010) (Cong et al., 2018) (Galbe et al., 2007) (Kiss, 2014). Continuous monitoring of the ethanol vapor pressure is vital to maintain product quality. As illustrated in Figure 5 the ethanol vapor pressure is gradually increased up to 50mmHg when the reactor temperature reaches 350K.

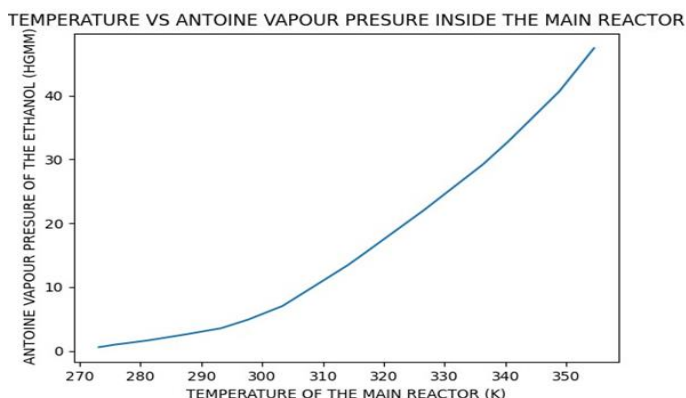


Figure 5. Changes in vapor pressure with the changing temperature in the main reactor

Vapor flow rate in the main reactor

Precise measurement of vapor flow rate of the ethanol in the main reactor during the distillation process is utmost important to provide critical insights into process performance and efficiency. According to the results, there are two peaks of high flow rate with a value of 0.90 Kg/min in 60th minute and 112th minute respectively. Vapor flow rate of the main reactor is illustrated in Figure 6.

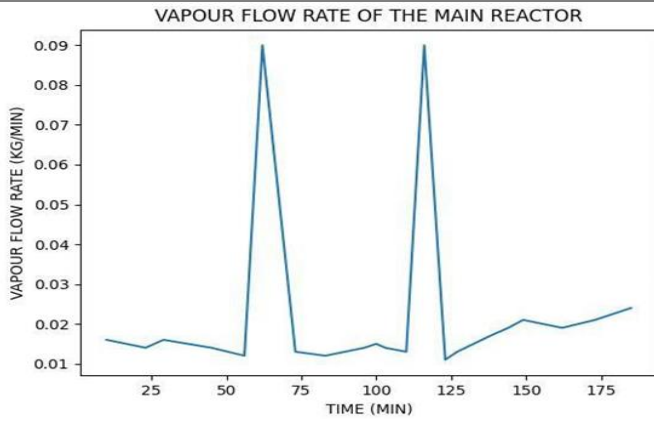


Figure 6. Vapor flow rate in the main reactor

Temperature sequence in the calandria reactor

Temperature monitoring in the Calandria reactor is facilitated by six thermocouples. According to the results, thermocouple 1 to 4 indicate relatively constant temperature around 90⁰C throughout the distillation process whereas thermocouples 5 and 6 indicate a low temperature around 10⁰C. Temperature distribution within the calandria reactor is illustrated in Figure 7.

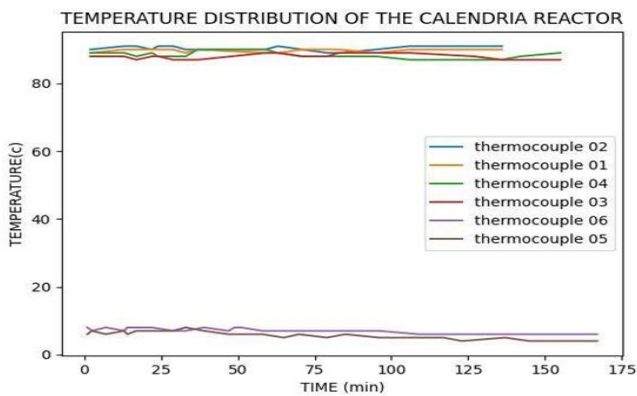


Figure7. Temperature sequence in the calandria reactor

Ethanol conversion ratio analyzing

Table 2. Conversion efficiency and comparison of final ethanol solutions

	Sample 01 (White Sugar)	Sample 02 (Ice Cream Bean)	Sample 03 (Jack Fruit)	STANDARD ETHANOL
Input Raw Ethanol Solution Quantity (L)	13	13	13	
Distilled Ethanol Quantity (L)	4.2	3.8	2.1	
Conversion Efficiency (%)	32.30	29.23	16.15	
Density (g/cm ³)	0.99	0.96	0.97	0.97
Dynamic Viscosity (mPs s)	2.21	2.11	2.02	1.18
Kynamatic Viscosity (mm ² /s)	2.22	2.18	2.08	1.22
pH	3.9	3.8	3.9	7.3

EC (mS/cm)	34.7	28.3	34.1	20-28
Ethanol % (w/w)	22	19.9	18.7	20

Physicochemical properties, such as viscosity, pH, and electrical conductivity, reveal that all biomass-derived ethanols differ from the standard in fluidity, acidity, and ionic content. The biomass samples showed higher viscosity, indicating residual organic compounds, and acidic pH levels (3.8–3.9) that may affect long-term stability and application. Elevated conductivity also suggests residual impurities, which may need removal to meet commercial ethanol standards. Despite these differences, White Sugar's balance of high ethanol yield and favorable characteristics positions it as a promising feedstock, with Ice Cream Bean as a secondary option, particularly in regions with limited access to White Sugar.

A comparison of different ethanol distillation methodologies are provided in Table 3 which shows satisfactory performances in the Novel system for the first distillation.

Table 3. Comparison of conversion efficiencies to the Novel vapor recompression method

Method	Efficiency (%)	Energy Demand	Cost-Effectiveness	Environmental Impact
Simple Distillation (Botshekan et al., 2022)	30-50%	High	Moderate	High energy and water usage
Fractional Distillation (E Silva & Miranda, 2021)	45-60%	High	Moderate	High due to water vapor
Azeotropic/Extractive (Miranda Nahieh Toscano et al., 2020)	70-80%	Very High	Costly	High due to chemical agents
Vapor Recompression	32.30 % (Max First pass)	Low to Moderate	Cost-effective long-term	Low (Yang et al., 2022)

CONCLUSION

The study demonstrated the effectiveness of a novel vapor recompression distillation unit in producing bioethanol from three feedstocks: White Sugar, Ice Cream Bean, and Jackfruit. White Sugar yielded the highest conversion efficiency at 32.31% and an ethanol concentration of 22% w/w, establishing it as the most suitable feedstock. In contrast, Ice Cream Bean and Jackfruit showed lower efficiencies of 29.23% and 16.15%, respectively.

The Coefficient of Performance (COP) for the system was calculated at 1.9851, indicating satisfactory energy efficiency in the distillation process. The acidic pH values of all samples suggested the presence of organic acids, which may affect product quality, while the higher viscosity compared to standard ethanol could impact processing.

Overall, the vapor recompression system demonstrates potential for improving the efficiency and sustainability of bioethanol production, contributing to cleaner fuel alternatives. Future research should focus on optimizing distillation parameters and exploring additional feedstocks to further enhance production efficiency and product purity.

REFERENCES

- Aditya, H. B., Mahlia, T. M. I., & Chong, W. T. (2016). Second generation bioethanol production: A critical review. *Renewable and Sustainable Energy Reviews*, 66, 631–653. <https://doi.org/10.1016/j.rser.2016.07.015>

2. Ansari, S., Soomro, A., Hussain, I., Solangi, U., & Sattar, A. (2016). PLC based Automatic Distillation and Collection of Ethanol-Water Solution. *Indian Journal of Science and Technology*, 9. <https://doi.org/10.17485/ijst/2015/v8i1/108655>
3. Arifeen, N., Wang, R., Kookos, I. K., Webb, C., & Koutinas, A. A. (2007). Process Design and Optimization of Novel Wheat-Based Continuous Bioethanol Production System. *Biotechnology Progress*, 23(6), 1394–1403. <https://doi.org/10.1021/bp0701517>
4. Arshad, M., Hussain, T., Iqbal, M., & Abbas, M. (2017). Enhanced ethanol production at commercial scale from molasses using high gravity technology by mutant *S. cerevisiae*. *Brazilian Journal of Microbiology*, 48, 403–409. <https://doi.org/10.1016/j.bjm.2017.02.003>
5. Botshekan, M., Moheb, A., Vatankhah, F., Karimi, K., & Shafiei, M. (2022). Energy saving alternatives for renewable ethanol production with the focus on separation/purification units: A techno-economic analysis. *Energy*, 239, 122363. <https://doi.org/10.1016/j.energy.2021.122363>
6. Bušić, A., Marđetko, N., Kundas, S., Morzak, G., Belskaya, H., Ivančić Šantek, M., Komes, D., Novak, S., & Šantek, B. (2018). Bioethanol Production from Renewable Raw Materials and Its Separation and Purification: A Review. *Food Technology and Biotechnology*, 56(3), 289–311. <https://doi.org/10.17113/ftb.56.03.18.5546>
7. Canales, E. R., & Marquez, F. E. (1992). Operation and experimental results on a vapor recompression pilot plant distillation column. *Industrial & Engineering Chemistry Research*, 31(11), 2547–2555. <https://doi.org/10.1021/ie00011a020>
8. Chen, J., Zhang, B., Luo, L., Yi, Y., & Shan, Y. (2021). A review on recycling techniques for bioethanol production from lignocellulosic biomass. *Renewable and Sustainable Energy Reviews*, 149, 111370. <https://doi.org/10.1016/j.rser.2021.111370>
9. Christian Oseto, T. J. G. (2020). *Insect Collection and Identification (Second)*. Academic Press.
10. Cong, H., Murphy, J. P., Li, X., Li, H., & Gao, X. (2018). Feasibility Evaluation of a Novel Middle Vapor Recompression Distillation Column. *Industrial & Engineering Chemistry Research*, 57(18), 6317–6329. <https://doi.org/10.1021/acs.iecr.8b00038>
11. Das, A., Paul, T., Jana, A., Halder, S. K., Ghosh, K., Maity, C., Mohapatra, P. K. D., Pati, B. R., & Mondal, K. C. (2013). Bioconversion of rice straw to sugar using multizyme complex of fungal origin and subsequent production of bioethanol by mixed fermentation of *Saccharomyces cerevisiae* MTCC 173 and *Zymomonas mobilis* MTCC 2428. *Industrial Crops and Products*, 46, 217–225. <https://doi.org/10.1016/j.indcrop.2013.02.003>
12. Dias, M., & Ensinas, A. (2009). Production of bioethanol and other bio-based materials from sugarcane bagasse: Integration to conventional bioethanol production process. *Chemical Engineering Research and Design*, 87(9), 1206–1216. <https://doi.org/10.1016/j.chemd.2009.06.020>
13. Dias, M., & Modesto, M. (2011). Improving bioethanol production from sugarcane: Evaluation of distillation, thermal integration and cogeneration systems. *Energy*, 36(6), 3691–3703. <https://doi.org/10.1016/j.energy.2010.09.024>
14. Duque, A., Álvarez, C., Doménech, P., Manzanares, P., & Moreno, A. D. (2021). Advanced Bioethanol Production: From Novel Raw Materials to Integrated Biorefineries. *Processes*, 9(2), Article 2. <https://doi.org/10.3390/pr9020206>
15. E Silva, M. P. G. D. C., & Miranda, J. C. D. C. (2021). Exergy efficiency of thermochemical syngas-to-ethanol production plants. *SN Applied Sciences*, 3(5), 534. <https://doi.org/10.1007/s42452-021-04526-3>
16. El-Sheekh, M. M., Bedaiwy, M. Y., El-Nagar, A. A., ElKelawy, M., & Alm-Eldin Bastawissi, H. (2022). Ethanol biofuel production and characteristics optimization from wheat straw hydrolysate: Performance and emission study of DI-diesel engine fueled with diesel/biodiesel/ethanol blends. *Renewable Energy*, 191, 591–607. <https://doi.org/10.1016/j.renene.2022.04.076>
17. Enweremadu, C. C., & Rutto, H. L. (2010). Investigation of Heat Loss in Ethanol-Water Distillation Column with Direct Vapour Recompression Heat Pump.
18. Errico, M., & Rong, B.-G. (2012). Synthesis of new separation processes for bioethanol production by extractive distillation. *Separation and Purification Technology*, 96, 58–67. <https://doi.org/10.1016/j.seppur.2012.05.022>
19. Galbe, M., Sassner, P., Wingren, A., & Zacchi, G. (2007). Process Engineering Economics of Bioethanol Production. In L. Olsson (Ed.), *Biofuels* (Vol. 108, pp. 303–327). Springer Berlin Heidelberg. https://doi.org/10.1007/10_2007_063
20. Gavahian, M., Farahnaky, A., & Sastry, S. (2016). Ohmic-assisted hydrodistillation: A novel method for

- ethanol distillation. Food and Bioproducts Processing, 98, 44–49. <https://doi.org/10.1016/j.fbp.2015.11.003>
21. Gavahian, M., Munekata, P. E. S., Eş, I., Lorenzo, J. M., Mousavi Khaneghah, A., & Barba, F. J. (2019). Emerging techniques in bioethanol production: From distillation to waste valorization. *Green Chemistry*, 21(6), 1171–1185. <https://doi.org/10.1039/C8GC02698J>
 22. Hargono, H., Jos, B., Purwanto, P., Sumardiono, S., & Zakaria, M. F. (2021). Fuel Grade Bioethanol Production from Suweg Starch Through Distillation-Adsorption Process Using Natural Zeolite. *IOP Conference Series: Materials Science and Engineering*, 1053(1), 012090. <https://doi.org/10.1088/1757-899X/1053/1/012090>
 23. Ishola, M., Jahandideh, A., & Haidarian, B. (2013). Simultaneous saccharification, filtration and fermentation (SSFF): A novel method for bioethanol production from lignocellulosic biomass. *Bioresource Technology*, 133, 68–73. <https://doi.org/10.1016/j.biortech.2013.01.130>
 24. Janousek, G. (2010). Evaluation of Ethanol and Water Introduction via Fumigation on Efficiency and Emissions of a Compression Ignition Engine Using an Atomization Technique. Department of Agricultural and Biological Systems Engineering: Dissertations, Theses, and Student Research. <https://digitalcommons.unl.edu/biosysengdiss/9>
 25. Kazemi, A., Hosseini, M., Mehrabani-Zeinabad, A., & Faizi, V. (2016). Evaluation of different vapor recompression distillation configurations based on energy requirements and associated costs. *Applied Thermal Engineering*, 94, 305–313. <https://doi.org/10.1016/j.applthermaleng.2015.10.042>
 26. Kiss, A. A. (2014). Distillation technology – still young and full of breakthrough opportunities. *Journal of Chemical Technology & Biotechnology*, 89(4), 479–498. <https://doi.org/10.1002/jctb.4262>
 27. Li, H., Liu, H., Li, Y., Nan, J., Shi, C., & Li, S. (2021). Combined Vapor Permeation and Continuous Solid-State Distillation for Energy-Efficient Bioethanol Production. *Energies*, 14(8), Article 8. <https://doi.org/10.3390/en14082266>
 28. Miranda Nahieh Toscano, Maciel Filho Rubens, & Wolf Maciel Maria Regina. (2020). Comparison of Complete Extractive and Azeotropic Distillation Processes for Anhydrous Ethanol Production Using Aspen Plus Simulator. *Chemical Engineering Transactions*, 80, 43–48. <https://doi.org/10.3303/CET2080008>
 29. Palacios-Bereche, R., Ensinas, A., Modesto, M., & Nebra, S. A. (2014). Mechanical Vapour Recompression Incorporated to the Ethanol Production from Sugarcane and Thermal Integration to the Overall Process Applying Pinch Analysis. *Chemical Engineering Transactions*, 39, 397–402. <https://doi.org/10.3303/CET1439067>
 30. Rosales-Calderon, O., & Arantes, V. (2019). A review on commercial-scale high-value products that can be produced alongside cellulosic ethanol. *Biotechnology for Biofuels*, 12(1), 240. <https://doi.org/10.1186/s13068-019-1529-1>
 31. Santos, E., Rostro-Alanis, M., & Parra-Saldivar, R. (2018). A novel method for bioethanol production using immobilized yeast cells in calcium-alginate films and hybrid composite pervaporation membrane. *Bioresource Technology*, 247, 165–173. <https://doi.org/10.1016/j.biortech.2017.09.091>
 32. Sarkar, N., Ghosh, S., & Bannerjee, S. (2012). Bioethanol production from agricultural wastes: An overview. *Renewable Energy*, 37(1), 19–27. <https://doi.org/10.1016/j.renene.2011.06.045>
 33. Singh, A., & Rangaiah, G. P. (2017). Review of Technological Advances in Bioethanol Recovery and Dehydration. *Industrial & Engineering Chemistry Research*, 56(18), 5147–5163. <https://doi.org/10.1021/acs.iecr.7b00273>
 34. Tgarguifa, A., Abderafi, S., & Bounahmidi, T. (2017). Modeling and optimization of distillation to produce bioethanol. *Energy Procedia*, 139, 43–48. <https://doi.org/10.1016/j.egypro.2017.11.170>
 35. Uday Bhaskar Babu, G., & Jana, A. K. (2014). Impact of vapor recompression in batch distillation on energy consumption, cost and CO₂ emission: Open-loop versus closed-loop operation. *Applied Thermal Engineering*, 62(2), 365–374. <https://doi.org/10.1016/j.applthermaleng.2013.09.057>
 36. Vacuubrand. (2018). Vapor Pressure Estimates Using Antoine Equation. VACUUBRAND. <https://vacuu-lan.com/vapor-pressure-estimates-antoine-equation/>
 37. Vohra, M., Manwar, J., & Manmode, R. (2014). Bioethanol production: Feedstock and current technologies. *Journal of Environmental Chemical Engineering*, 2(1), 573–584. <https://doi.org/10.1016/j.jece.2013.10.013>